EXPERIMENT ON THE PERFORMANCE OF A DEFORMED GEAR HOLE-PRICKING MECHANISM

Jinlong Feng, Xianglan Ming*, Qichao Li, Hua Li

The hole-pricking mechanism is the key component of deep application liquid fertilizer machine. In order to obtain the hole-pricking mechanism with better performance, the deformed gear hole-pricking mechanism was designed and a deformed gear hole-pricking test-bed was developed. Taking the single-factor and orthogonal rotation test scheme, the planetary carrier speed and trolley speed as the test factors, the hill width and hill distance as the test indexes, the orthogonal rotation test data were analyzed and optimized by using the Design-Expert 7.0.0 software. The optimum results were 80 r/min of the rotating speed of the planet carrier, 0.60 m/s of the test trolley speed, 220 mm of the output hole distance was and 22.8 mm of the hole mouth width. It meets the requirements of the hole-pricking performance of the liquid fertilizer applicator, and the test results also meet the agronomic requirements.

Key words: deformed gear; hole-pricking mechanism; hole width; hole distance; test optimization

1. Introduction

Deep application liquid fertilizer is an agricultural fertilization technology that applies liquid fertilizer deep into the soil layer near the crop root. It has the characteristics of accelerating crop absorption and improving crop yield and quality. This technology can give consideration to agricultural economic and ecological benefits and promote sustainable agricultural development [1-2]. The research and development of deep application liquid fertilizer applicator is a necessary condition for the application of this technology. Currently, the hole-pricking mechanism of deep application liquid fertilizer applicator mainly has four structures: crank and rocker, elliptical gear, full elliptical gear and Bessel gear. The track of crank and rocker hole-pricking mechanism is too forward when it enters the soil. This makes the inertial force of the mechanism difficult to control and the vibration intensifies, resulting in large hole opening and serious soil returning of fertilizer spraying needle [3]. Through kinematic and dynamic optimization, although the hole-pricking number of elliptical gear hole-pricking

*College of Mechanical and Electrical Engineering, Lingnan Normal University, Zhanjiang 524048, China
*Email: 37002165@qq.com

mechanism has improved, but the machines and tools still have great vibration and large hole opening [4]. The full elliptical gear hole-pricking mechanism has simple structure and high hole binding efficiency, but the hole opening is large [5-7]. Bessel gear hole-pricking mechanism can realize high-speed hole-pricking with less vibration. It is composed of seven Bessel gears. Although the hole size has been improved, and the structure is complex and the machining precision is high. It is difficult to realize the characteristics of Bessel gear transmission [8-10]. As such, a deformed gear hole-pricking mechanism was proposed in this paper. The deformed gear planetary gear train of the mechanism was simple in structure and easy to process to meet the characteristics of non-uniform transmission. According to adjusting the deformation coefficient and eccentricity of the deformed gear, the longitudinal and transverse changes of the transmission ratio can be realized, and the adjustable range of the transmission ratio can be increased. Using the characteristics of the transmission, the mechanism can get smaller holes. The indoor bench test is carried out for the deformed gear hole-pricking mechanism, and a more reasonable combination of working parameters is found through the test. This provides a reference basis for the design and optimization of deep application liquid fertilizer applicator.

2. Structure and Working Principle of Deformed Gear Hole-Pricking Mechanism

The structure of deformed gear hole-pricking mechanism is shown in Fig. 1, which is mainly composed of five equal deformed gears, planet carrier, rocker arm and fertilizer spraying needle. The rotation center of each deformed gear was located at its focus. Two pairs of deformed gears were arranged at both ends of the long shaft of the central deformed sun gear 4, respectively. The planet carrier 1 was coaxial with the central deformed gear 4. The rocker arm 2 was consolidated with the planetary deformed gear 6, and the fertilizer spraying needle was assembled and fixed at one end of the rocker arm.

The power is input through the deformed sun axle fixedly connected with the planet carrier. The deformed gear 4 is fixedly connected with the frame, which is in a static state during operation and does not rotate with the rotation of the planet carrier. When the intermediate deformation gear 5 works, it revolves around the axis of the planet carrier and rotates around the axis fixed on the planet carrier at the same time. The planetary deformation gear 6 also revolves around the axis of the planetary carrier along. At the same time, it rotates around the axis fixed on the planetary carrier to form the trajectory of the fertilizer spraying needle tip.

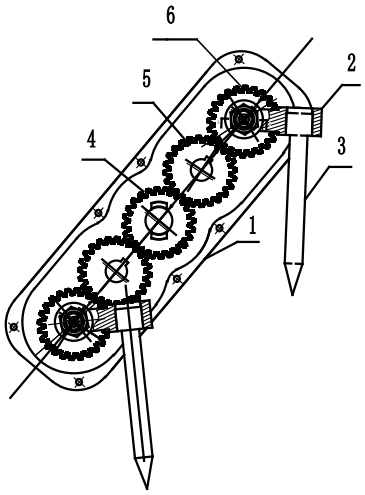

Fig.1 Structural diagram of deformed gear deep construction mechanism
1. Planet carrier; 2. Rocker; 3. Fertilizer spraying needle; 4. Deformed sun gear; 5. Upper intermediate deformed gear; 6. Upper planetary deformation gear

3. Performance Test of Deformed Gear Hole-Pricking Mechanism

3.1 Test Device

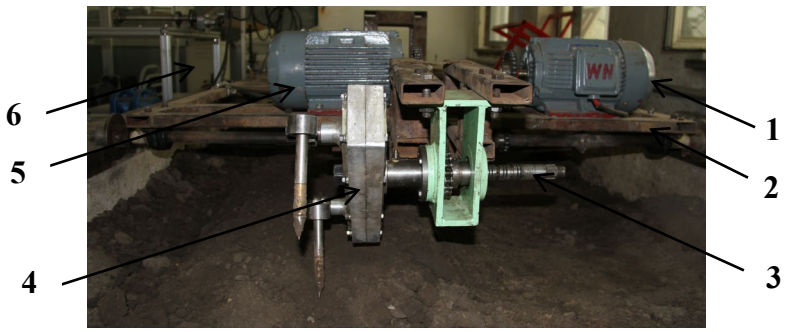

Fig.2 Test bench for deformed gear hole-pricking mechanism
1. Motor I; 2. Test trolley; 3. Transmission; 4. Deformed gear hole-pricking mechanism; 5. Motor II; 6. Frequency conversion cabinet

In order to further verify the effect of the deformed gear hole-pricking mechanism and its reliability in practical work, the mechanism is processed and a field simulation test is carried out on the independently designed test-bed. The structure of the test-bed is shown in Fig. 2. Motor I controls the test trolley to move back and forth on the soil groove guide rail. Motor II controls the rotation of the deformed gear hole-pricking mechanism through the transmission device. The

liquid fertilizer deep injection mechanism rotates once to complete the hole-pricking movement twice. The frequency of motor I and motor II is controlled by the frequency converter to realize the speed change of the test trolley and planet carrier.

3.2 Test Design

The width and distance of holes are the indexes to evaluate the performance of the hole-pricking mechanism. The main working parameters affecting the hole-pricking performance are planet carrier speed and trolley speed. The above two factors are determined as the test factors of hole-pricking performance. Singe-factor and two-factor five-level quadratic rotation orthogonal experimental designs were adopted, and the experimental coding table is shown in Table 1. The Design expert 7.0.0 software was used to process the experimental data, and the influence law of various factors on the width and distance of holes of the deep fertilizer mechanism was analyzed [11-13].

Table 1

Code table of test level

Code value	Test trolley speed /m·s^{-1}	Planetary carrier speed /r·min^{-1}
Upper asterisk arm(1.414)	0.67	94
Upper level(1)	0.65	90
Zero level(0)	0.60	80
Lower level(-1)	0.55	70
Lower asterisk arm(-1.414)	0.53	66

4. Results and Analysis

4.1 Single-Factor Test

4.1.1 Influence of Trolley Speed on Hole Width

When the speed of planet carrier was 80 R/min, the five levels of test factors were 0.50 m/s, 0.55 m/s, 0.60 m/s, 0.65 m/s and 0.70 m/s, respectively. Repeat the test for 5 times at each level and the Design-Expert 7 0.0 software was used to analyze the test data and obtain the influence curve of the test trolley speed on the hole width, as shown in Fig. 3

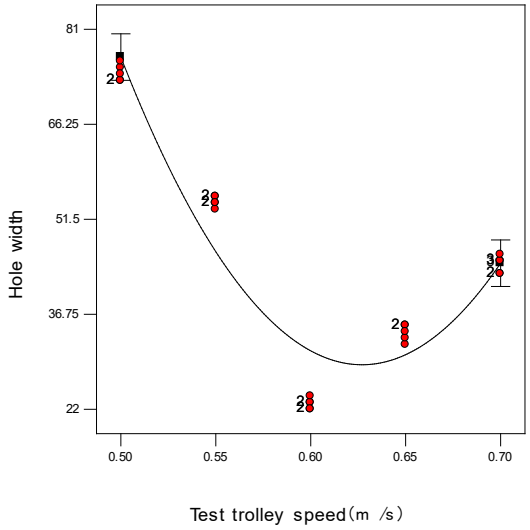

Fig. 3 Effect of the trolley speed on hole width

It can be seen from Fig.3, when the planet carrier speed is constant and the test trolley speed changes in the range of 0.5-0.6 m/s, the hole width decreased with the increase of speed. The reason is that during the hole-pricking process, the fertilizer spraying needle has the implicated speed that is consistent with the speed direction of the test trolley and changes with the test trolley speed. It also has the relative speed generated with the rotation of the planet carrier. When the rotation speed of the planet carrier is a fixed value, the relative speed of the fertilizer spraying needle remains unchanged. When the test trolley speed changes in the range of 0.5-0.6 m/s, the implicated speed of the fertilizer spraying needle gradually increases with the increase of test trolley speed and gradually approaches the relative speed. Therefore, the hole width during the hole- pricking also decreases gradually. When the test trolley speed is in the range of 0.6-0.7 m/s, the implicated speed of the fertilizer spraying needle continues to increase with the increase of test trolley speed. At this time, the implicated velocity is greater than the relative velocity, and the hole width increases gradually with the increase of velocity difference.

4.1.2 Influence of Planet Carrier Speed on Hole Width

When the test trolley speed was 0.6 m/s, the influence of planet carrier speed on hole width was studied. The five levels of test factors were 60 r/min, 70 r/min, 80 r/min, 90 r/min and 100 r/min, respectively. Repeat the test for 5 times, and the Design-Expert7.00 software was used to analyze the test data and obtain the influence curve of the planet carrier speed on hole width, as shown in Fig. 4.

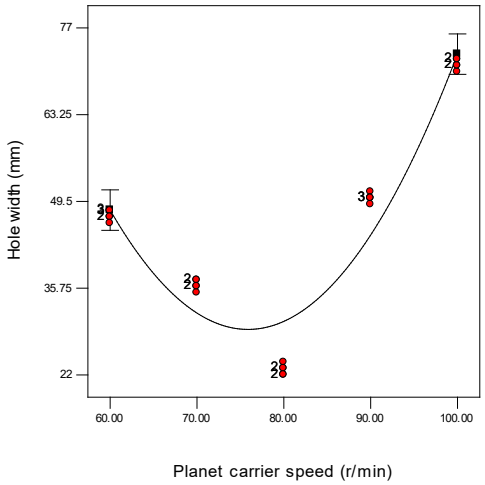

Fig. 4 Influence of planet carrier speed on cavity width

It can be seen from Fig. 4 that when the test trolley speed is constant and the planet carrier speed changes in the range of 60-80 r/min, the hole width decreases with the increase of planet carrier speed. The reason is that within this range, the relative speed of the fertilizer spraying needle is less than its involved speed, and the speed difference gradually decreases with the increase of rotating speed. Therefore, the hole width decreased with the increase of rotating speed. When the planet carrier speed changes in the range of 80-100 r/min, the hole width increases with the increase of planet carrier speed. The reason is that within this range, the relative speed of the fertilizer spraying needle is greater than its implicated speed, and the speed difference increases gradually with the increase of the rotating speed. Therefore, the hole opening width of the hole-pricking process increases with the increase of the rotation speed.

4.1.3 Influence of the test trolley speed on hole distance

When the speed of planet carrier was 80 r/min, the influence of test trolley speed on hole distance was studied. The five levels of test factors were 0.50 r/min, r/min, 0.6 m/s, 0.65 m/s and 0.70 m/s, respectively. Five repeated tests were conducted at each level, and 25 tests in total. The Design-Expert7.00 software was applied to analyze the test data and obtain the influence curve of the test trolley speed on hole distance, as shown in Fig. 5.

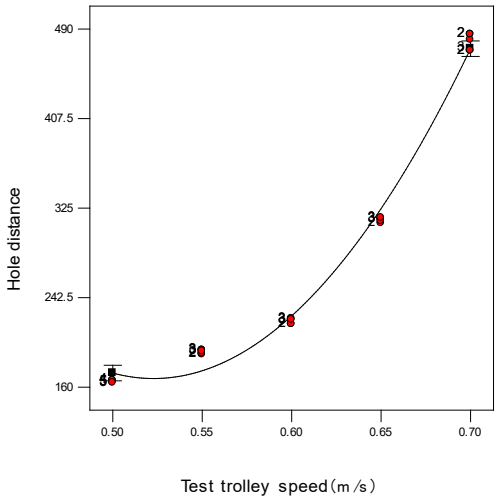

Fig.5 Influence of test trolley speed on hole distance

It can be seen from Fig. 5 that when the planetary carrier speed is constant and the test trolley speed changes in the range of 0.5-0.7 m/s, the hole distance increases with the increase of the test trolley speed. This is because when the length of the test soil tank is constant, the time taken for the test trolley to pass decreases with the increase of speed. Therefore, when the rotation speed of the planet carrier and the traveling distance of the trolley remain unchanged, the pricking holes will gradually decrease with the decrease of time. The decrease of the pricking holes will lead to the increase of hole distance. Therefore, the hole distance will gradually increase with the increase of the speed of the test trolley.

4.1.4 Influence of Planet Carrier Speed on Hole Distance

When the test trolley speed was 0.60 m/s, the influence of planet carrier speed on hole distance was studied. The five levels of test factors were 60 r/min, 70 r/min, 80 r/min, 90 r/min and 100 r/min, respectively. Five repeated tests were conducted at each level, and 25 in total. The Design-Expert 7.00 software was applied to analyze the test data and obtain the influence curve of planet carrier speed on hole distance, as shown in Fig. 6.

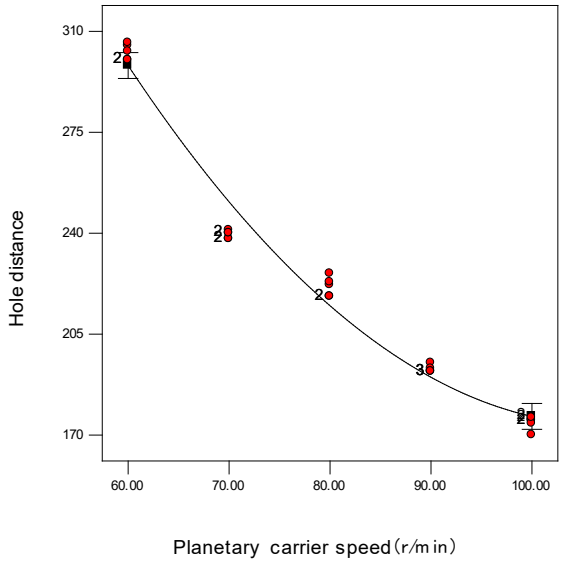

Fig. 6 Influence of the planet carrier speed on hole distance

It can be seen from Fig. 6 that when the test trolley speed is constant and the planet carrier speed changes in the range of 60-100 r/min, the hole distance decreases with the increase of planet carrier speed. Since the speed of the trolley and the length of the test soil tank are constant, the time taken for the test trolley to pass is constant. Therefore, when the test trolley speed and the trolley travel distance remain unchanged, the hole-pricking increases gradually with the increase of the planet carrier speed. Increasing the number of pricking holes will lead to the decrease of hole distance, and the hole distance will gradually decrease with the increase of planet carrier speed.

4.2 Multi-factor test

Based on the single factor, the orthogonal rotation test was carried out. The test scheme and results are shown in Table 2. The Design-Expert 7.0.0 was used to analyze the test data in Table 2. The response surface of the influence of the test trolley speed and planetary carrier speed on hole width and hole distance is obtained as shown in Fig. 7 and Fig. 8. The multi-factor analysis of variance is shown in Table 3 and Table 4 [14-16].

Table 2

Quadratic rotation orthogonal test scheme and results

No.	Factors		Performance indexes	
	Test trolley speed x_1/m·s^{-1}	Planetary carrier speed x_2/r·min^{-1}	Hole width y_1/mm	Hole distance y_2/mm
1	-1	-1	57	253
2	-1	1	39	207
3	1	-1	71	365
4	1	1	62	224
5	0	-1.414	73	298
6	0	1.414	50	171
7	-1.414	0	48	162
8	1.414	0	66	415
9	0	0	22	218
10	0	0	22	221
11	0	0	23	218
12	0	0	25	219
13	0	0	22	222
14	0	0	25	222
15	0	0	23	224
16	0	0	23	221

When the significance level is $F_{0.05}$, it can be seen from Table 3 that x_1, x_2, x_1^2, x_2^2 and x_1x_2 have a significant impact on the hole width, which are the valid items of the model. After removing the insignificant items, the fitted regression equation is as follows:

$$y_1 = 3737.9 - 33.3x_2 - 8093.9x_1 + 4.5x_1x_2 + 0.19x_2^2 + 6575x_1^2 \quad (1)$$

Table 3

Variance analysis of the influence of various factors on the width of holes

Source	Sum of squares	Freedom	F value	Significance(P>F)
Model	5906.09	5	300.17	< 0.0001
x_2	442.93	1	112.56	< 0.0001
x_1	487.59	1	78.91	< 0.0001
x_2^2	2793.78	1	709.95	< 0.0001
x_1^2	2161.53	1	549.28	< 0.0001
x_1x_2	20.25	1	5.15	0.0467
Error	39.35	10		
Total	5945.44	15		

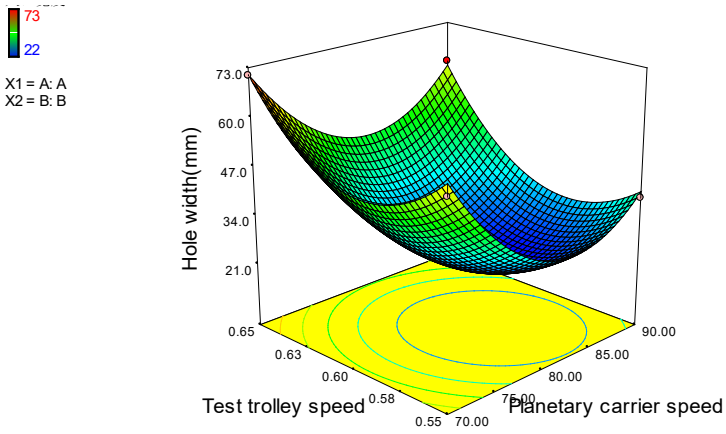

Fig. 7 Response surface diagram of the influence of test trolley speed and planetary carrier speed on hole width

It can be seen from Fig. 7 that when the test trolley speed is constant and the planet carrier speed changes in the range of 70-90 r/min, the hole width decreases first and then increases gradually with the increase of the planet carrier speed. When the planet carrier speed is constant and the test trolley speed changes in the range of 0.55-0.65 m/s, the hole width first decreases and then increases with the increase of test trolley speed. The response surface changes faster along the speed direction of the planet carrier than that of the test bench. It can be seen from Table 3 that the F value of the effect of planet carrier speed on the hole width y_1 is 112.56 and that of test trolley speed on the hole width y_1 is 78.91. Therefore, the effect of planet carrier speed on the cavity width is greater than that of test trolley speed.

When the significance level is $F_{0.05}$, it can be seen from Table 5 that x_1, x_2, x_1^2 and x_1x_2 have a significant impact on the hole width, which is a valid item of the model. After removing the insignificant items, the fitted regression equation is:

$$y_2 = 3131.24 + 5.97x_2 - 11505.99x_1 - 14.50x_1x_2 + 11700x_1^2 \qquad (2)$$

Table 4

Analysis of variance of influence of various factors on hole distance

Source	Sum of squares	Freedom	F value	Significance(P>F)
Model	50787.53	5	347.60	< 0.0001
x_2	5934.75	1	203.09	< 0.0001
x_1	37757.53	1	1292.09	< 0.0001
x_2^2	40.50	1	1.39	0.2664
x_1^2	6844.50	1	234.22	< 0.0001
x_1x_2	210.25	1	7.19	0.023
Error	4405.65	10		
Total	64983	15		

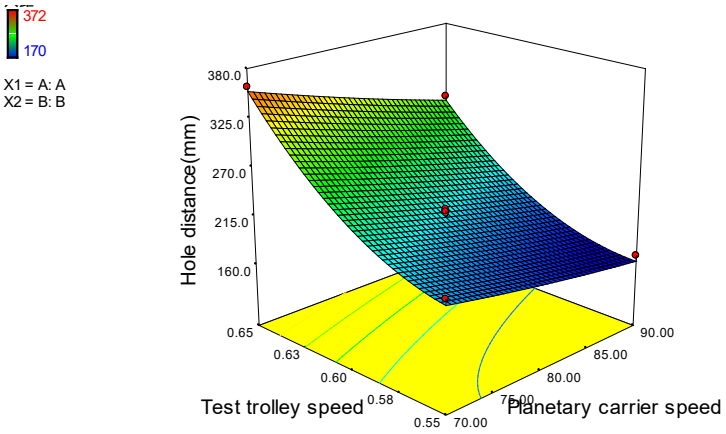

Fig. 8 Response surface diagram of the influence of test trolley speed and planetary carrier speed on hole distance

It can be seen from Fig. 8 that when the test trolley speed is constant and the planet carrier speed changes in the range of 70-90r/min, the hole distance gradually decreases with the increase of the planet carrier speed. When the planet carrier speed is constant and the test trolley speed changes in the range of 0.55-0.65m/s, the hole distance increases gradually with the increase of test trolley speed. The response surface changes slowly along the speed direction of the planet carrier than that of the test bench. It can be seen from Table 4 that the effect of planet carrier speed on hole distance y_2 is 203.09, and the F value of the effect of the test trolley speed on the hole distance y_2 is 1292.09. Therefore, the effect of test trolley speed on hole distance y_2 is greater than that of planet carrier speed.

4.3 Test Optimization and Verification

In order to obtain the best parameter level combination of test trolley speed and planetary carrier speed, taking the hole distance and hole width as the performance index and the constraint conditions required by agronomy as the boundary conditions, the regression equation of hole distance and hole width is analyzed. The nonlinear programming mathematical model is obtained as follows:

$$\begin{cases} y_1 \in [20,30] \\ y_2 \in [210,230] \\ s.t \quad 0.55 \le x_1 \le 0.65 \\ 70 \le x_2 \le 90 \\ 0 < y_1 \le 1 \\ 0 < y_2 \le 1 \end{cases} \tag{3}$$

Among them, the objective function used in parameter optimization is:

$$\begin{cases} y_1 = 3737.9 - 33.3x_2 - 8093.9x_1 + 4.5x_1x_2 + 0.19x_2^2 + 6575x_1^2 \\ y_2 = 3131.24 + 5.97x_2 - 11505.99x_1 - 14.50x_1x_2 + 11700x_1^2 \end{cases} \tag{4}$$

Using the Design-Expert 7.0.0 software to optimize the parameters, the best parameter combination scheme of test trolley speed and planetary carrier speed can be obtained, that is, the planetary carrier speed is 80 r/min; the test trolley speed is 0.60 m/s, the output hole distance is 220 mm and the hole width is 22.8 mm. This meets the requirements of hole-pricking performance.

Table 5

Verification test results

Test	Factors		Performance indexes	
	trolley speed x_1 /m·s^{-1}	Planetary carrier speed x_2 /r·min^{-1}	Hole width y_1 /mm	Hole distance y_2 /mm
	0.62	80	23	220
			24	220
			21	220
			22	220
			21	220

Five groups of verification tests were carried out with the optimal plan planet carrier speed of 80 r/min and the test rig speed of 0.60 m/s. The verification results are shown in Table 5. It can be seen that the in the test results, the maximum hole width is 24 mm; the minimum is 21 mm, and the average value of these five groups of verification tests is 22.2 mm. The results show that the optimal working parameter combination of test trolley speed and planetary carrier speed can meet the agronomic requirements of hole width and hole distance.

5. Conclusion

(1) In this paper, a test-bed for the hole piercing mechanism of deformed gear was established and a single factor test was designed. The results show that the hole width decreased and then increased with the increase of test trolley speed, and also decreased and then increased with the increase of planet carrier speed. The hole distance increased with the increase of test trolley speed, and decreased with the increase of planet carrier speed.

(2) Using the quadratic orthogonal rotation combination design test, the mathematical model of the performance index and test factors of hole-pricking was established, and the influence of the interaction relationship on the index of pricking point was analyzed.

(3) The Design-Expert 7.0.0 software was used to analyze and optimize the test results. The results showed that the hole pricking performance was optimal when the travel star frame speed was80 r/min and the test trolley speed was 0.60 m/s, that is, the travel star frame speed was 80 r/min; the test trolley speed was 0.60 m/s; the output hole distance was 220 mm and the hole width was 22.8 mm.

Acknowledgments

Thank you for Postdoctoral Science Foundation of Heilongjiang Province of China (Grant No. LBH-Z18254), Guangdong basic and applied basic research fund project (2021A1515011790), Special project for doctoral talents of Lingnan Normal University (ZL2021019), Innovation team of intelligentially and key technology research for agricultural machinery and equipment in Western of Guangdong province (2020KCXTD039).

REFERENCES

[1] *da Silva, M. J., & Magalhaes, P. S.,* A liquid injection dosing system for site-specific fertilizer management. Biosystems Engineering, vol. 163, pp. 150-158, 2017. https://doi.org/10.1016/j.biosystemseng.2017.09.005

[2] *da Silva, M. J., Franco, H. C. J., & Magalhães, P. S. G.,* Liquid fertilizer application to ratoon cane using a soil punching method. Soil &Tillage Research, vol. 165, pp. 279-285, 2017. https://doi.org/10.1016/j.still.2016.08.020

[3] *Dixit, J., Kumar, V., & Ali, M.,* Development and Evaluation of a Single Row Manual Vegetable Transplanter. Agricultural Engineering Today, vol. 42, no. 2, pp. 58-66, 2018.

[4] *Fan C.J., Xiong G.M., Zhou M.F.,* Application and advancement of ADAMS. Beijing: China Machine Press, 2006.

[5] *Thomas, E. V.,* Development of a mechanism for transplanting rice seedlings. Mechanism and Machine Theory, vol. 37, no. 4, pp. 395-410, 2002. https://doi.org/10.1016/S0094-114X(01)00071-4

[6] *Jo, J. S., Okyere, F. G., Jo, J. M., & Kim, H. T.,* A study on improving the performance of the planting device of a vegetable transplanter. Journal of Biosystems Engineering, vol. 43, no. 3, pp. 202-210, 2018. https://doi.org/10.5307/JBE.2018.43.3.202

[7] *Otto, R., Franco, H. C. J., Faroni, C. E., Vitti, A. C., de Oliveira, E. C. A., Sermarini, R. A., & Trivelin, P. C. O.,* The role of nitrogen fertilizers in sugarcane root biomass under field conditions. Agricultural Sciences, vol. 5, no. 14, pp. 1527-1538, 2014. DOI: 10.4236/as.2014.514164

[8] *Wang J.F., Wang J.W., Ju J.Y., He J.N.,* Research progress on pricking hole mechanism of deep-fertilization liquid fertilizer applicator. Journal of Northeast Agricultural University, vol. 44, no. 5, pp. 157-160, 2013. DOI: 10.19720/j.cnki.issn.1005-9369.2013.05.030

[9] *Vieira-Megda, M. X., Mariano, E., Leite, J. M., Franco, H. C. J., Vitti, A. C., Megda, M. M., Khan, S.A., Mulvaney, R.L., Trivelin, P. C. O.,* Contribution of fertilizer nitrogen to the total nitrogen extracted by sugarcane under Brazilian field conditions. Nutrient Cycling in Agroecosystems, vol. 101, no. 2, pp. 241-257, 2015. https://doi.org/10.1007/s10705-015-9676-7

[10] *Wang J.W., Zhou W.Q., Bai H.C., Wang J.F., Huang H.N., Wang Z.B.,* Design and experiment of differential-type bidirectional distribution device for fertilizer supply for deep-fertilizer liquid fertilizer application. Transactions of the Chinese Society for Agricultural Machinery, vol. 49, no. 6, pp. 105-111, 2018. DOI: 10.6041/j.issn.1000-1298.2018.06.012.

[11] *Wang J.W., Zhou W.Q., Wang X., Li X., Wang J.L., Li S.W.,* Oblique type pricking hole mechanism based on Lagrange curve for cubic fitting trajectory. Transactions of the Chinese Society for Agricultural Machinery, vol. 48, no. 5, pp. 79-85, 2017. DOI:10.6041/j.issn1000-1298.2017.05.009.

[12] *Xu X.H., He M.Z.,* Experimental design and application of Design-Expert and SPSS. Beijing: Science Press, 2010.

[13] *Zhang, L., Cai, Z., Wang, L., Zhang, R., & Liu, H.,* Coupled Eulerian-Lagrangian finite element method for simulating soil-tool interaction. Biosystems Engineering, vol. 175, pp. 96-105, 2018. https://doi.org/10.1016/j.biosystemseng.2018.09.003

[14] *Zhang, L. B., Cai, Z. X., & Liu, H. F.,* A novel approach for simulation of soil-tool interaction based on an arbitrary Lagrangian–Eulerian description. Soil and Tillage Research, vol. 178, pp. 41-49, 2018. https://doi.org/10.1016/j.still.2017.12.011

[15] *Zhao Y., Yu G.H., Wu C.Y.,* Numerical analysis and synthesis of mechanism. Beijing: China Machine Press, 2005.

[16] *Zhou, C., Hu, B., Chen, S., & Ma, L.,* Design and analysis of high-speed cam mechanism using Fourier series. Mechanism and Machine Theory, vol. 104, pp. 118-129, 2016. https://doi.org/10.1016/j.mechmachtheory.2016.05.009